ELSEVIER

Journal of Photochemistry and Photobiology A: Chemistry 121 (1999) 27–36

Journal of Photochemistry and Photobiology A:Chemistry

A tetra-(bipyridylphenyl)porphyrin for luminescence sensing of divalent metal ions

Rachael A. Kipp*, Yinquin Li, Jerald A. Simon, Russell H. Schmehl

Department of Chemistry, Tulane University, New Orleans, LA 70118, USA

Received 16 October 1998; accepted 12 November 1998

Abstract

The fluorescence quenching of a tetra-(bipyridylphenyl)porphyrin (**1a**) by various metal ions in DMSO solutions is discussed. In all cases quenching results via formation of a ground state complex between a bipyridyl moiety of the porphyrin and the metal ion. For Zn(II) tetra-(bipyridylphenyl)porphyrin (**1b**) luminescence quenching is only observed with Co(II), Ni(II) and Cu(II). In all three detectable quenching is observed at sub-part per million concentrations. For luminescent species having multiple, independent, metal ion binding sites (like **1b**), detailed examination of the luminescence quenching clearly shows that association equilibria for binding metal ions at atleast two of the available sites must be taken into account. The quenching of **1b** with Cu(II) was examined in detail and the rate constant for quenching was determined using picosecond time resolved absorption spectrophotometry. The mechanism of the quenching process is discussed in each case. Metal ion selectivity is obtained for this system as a result of both thermodynamic and kinetic limitations to quenching the luminescence of **1b**.

Keywords: Tetra-(bipyridylphenyl)porphyrin; Luminescence quenching; Metal ions

1. Introduction

One approach for developing luminescence sensors for metal ions involves the use of supramolecular ensembles containing an emissive chromophore that is covalently linked to a ligand which binds the ion of interest. The mode of sensing in such systems may involve either an increase in luminescence from the chromophore upon ion association or, more often, luminescence quenching [1–4]. Sensing can occur by several mechanisms including energy transfer, electron transfer, [5] the enhancement of intersystem crossing (to produce an excited state of a different spin) [6] and net chemistry to yield emissive or non-emissive products [7–9].

Most luminescent sensors involving energy or electron transfer reactions contain three essential components: a chromophore (C), a receptor for the ion(s) of interest (R) and a covalent unit bridging the chromophore and receptor (B). A goal in the design of C–B–R systems is to employ a chromophore which is not affected by the presence of quenching species that are abundant in the environment (i.e. O_2), but is readily quenched upon association of the ion of interest. For quenching processes involving intramolecular exchange energy transfer or electron transfer, the rate constant depends on the magnitude of electronic coupling interactions through the bridge. Thus, the structure of the bridging unit has a large impact on the change in luminescence observed for the chromophore. For effective sensing, the rate constant for the intramolecular quenching process must be much larger than the rate constants for radiative and non-radiative decay. Also, since quenching reactions of substances that do not bind to the receptor are bimolecular, it is advantageous to employ chromophores with very short luminescence lifetimes (very rapid radiative decay rate constants) to minimize bimolecular reactions. Thus, optimal systems will have chromophores with very short excited state lifetimes, high emission quantum yields for the unquenched form, and strong electronic coupling through the bridge to maximize the quenching rate constant.

Selectivity in sensing is most easily achieved by employing a receptor which is specific for a particular substrate. An alternative approach is to use a somewhat less selective binding unit and gain selectivity through differences in both binding equilibria and quenching efficiencies of different ions. For metal ion sensing, the second approach involves using a relatively non-selective ligand attached to a chromophore and relying on the quenching reaction to achieve selectivity. An obvious disadvantage of this approach is that the degree of quenching at any given concentration of the ion

*Corresponding author.

1010-6030/99/$ – see front matter
PII: S1010-6030(98)00445-6

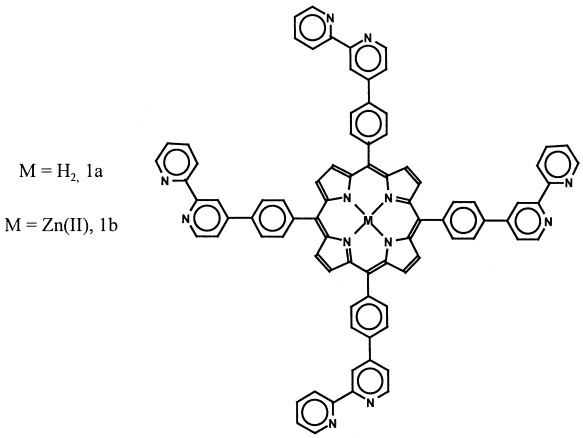

Fig. 1. Porphyrins **1a** and **1b**.

of interest will be influenced by other metal ions present that competitively associate with the receptor ligand. An advantage is that the luminescence of the C–B–R assembly can be restored if the quenching ion can be displaced from the receptor by exposure to high concentrations of non-quenching ions capable of competing for receptor sites.

In this work we present an investigation of fluorescence quenching of the Zn(II) complex of tetra-(4-(2,2′-bipyrid-4-yl)phenyl)porphyrin (**1b**) (Fig. 1), by various divalent and trivalent metal ions in DMSO solutions. The mechanism of quenching is investigated for Cu(II), Co(II) and Ni(II) and issues relating to binding equilibria are also addressed. The results indicate that quenching is most effective for metal ions capable of quenching the porphyrin singlet excited state by electron transfer and that energy transfer and heavy atom induced fluorescence quenching pathways are relatively unimportant. Rate constants for intramolecular quenching are measured to be $>10^9\ s^{-1}$ for those ions that serve as effective quenchers.

2. Experimental

2.1. Materials used

p-Tolualdehyde, pyruvic acid sodium salt, iodine, ammonium acetate, ceric ammonium nitrate, pyrrole, propionic acid, and dimethyl sulfoxide were purchased from Aldrich and/or Fisher Chemical and were used as received. Ammonium hexafluorophosphate, NH_4PF_6, was synthesized by the addition of one equivalent of HPF_6 to one equivalent of NH_4OH in ethanol. The white precipitate was collected by filtration and dried in a vacuum. Other reagents and solvents were reagent grade or better.

2.2. Syntheses

2.2.1. 4-(3-Carboxy-3-oxo-prop-1-en-yl) toluene (**2**)

This reaction is a modification of the preparation by Rheimer [10]. A solution of *p*-tolualdehyde (5 g, 0.042 mol) in ethanol (40 ml) was added to a rapidly stirred and cooled solution of sodium pyruvate (7 g, 0.063 mol) in water (100 ml) in a 500 ml beaker which was immersed in an ice bath. The resulting white suspension was stirred vigorously for 2 min, followed by the addition of 10 ml of 10% NaOH (aq). The solution became light yellow and clear after 3–5 min. The reaction was allowed to continue at room temperature for an additional 40 min, while bright yellowish precipitate formed. The solution was then acidified with 5% HCl (aq) to pH 3–4 and stirred for 5 min. The resulting precipitate was filtered and washed in sequence with water and ethanol (20 ml). The solid was dried in vacuum to yield 4.7 g (61%). The reaction was repeated several times and yields ranged from 40–80%. The crude product was recrystallized from water. mp 129–130°C. HRMS ($C_{11}H_{10}O_3$): 190.06229 (dev. 0.01 ppm), peaks: 144(100), 114(27), 91(13). IR $\nu_{co} = 1712,\ 1683\ cm^{-1}$. ^1H NMR ($CDCl_3$): 8.12(d, 1H), 7.58(d, 1H), 7.55(d, 1H), 7.25(d, 1H), 2.38(s, 3H).

2.2.2. 2-Acetylpyridinepyridinium hexafluorophosphate (**3**)

This salt was made by a modified literature procedure [11]. Iodine (40.8 g, 0.148 mol) was dissolved in pyridine (120 ml), and added to 2-acetylpyridine (16.56 ml, 0.148 mol) in pyridine (40 ml). The solution was refluxed at 120°C for 2.5 h and then allowed to sit for 12 h. The dark precipitate that formed was collected, redissolved in hot water (500 ml), charcoal (5–8 g) was added, the solution was heated (50–100°C) for 10 min, and the charcoal was removed by filtration. The product was precipitated as the hexafluorophosphate salt by the addition of saturated aqueous NH_4PF_6 to the filtrate to yield 38.40 g (92.7%). ^1H NMR (CD_3COCD_3): 9.18(d, 2H), 8.83(d, 1H), 8.80(t, 1H), 8.40(t, 2H), 8.10(m, 2H), 7.80(m, 1H), 6.74(s, 1H). FAB/MS: ($C_{12}H_{11}N_2OPF_6$): 199.1 (M-PF_6).

2.2.3. p-(2,2′-Bipyrid-4-yl)toluene (**4**)

A suspension of **2** (3.0 g, 0.016 mol), **3** (8.12 g, 0.023 mol), and ammonium acetate (27.10 g, 0.352 mol) in water (250 ml) was refluxed at 100–110°C in an oil bath for 3 h. The hot solution was then filtered and the precipitate was washed with water and then air-dried to yield 7.2 g (96%) of the carboxylate. The crude product (1.5 g) was heated in a sublimator at 140–160°C under vacuum to effect decarboxylation. The sublimed product was collected (1.2 g) and purified by redissolving in chloroform–triethylamine (20 : 1), filtering, evaporating the solution to dryness, and then chromatographing on a silica gel (10 × 4.5 cm, $CHCl_3$) column. The light blue fluorescent band was eluted with chloroform–acetone (20 : 1) to yield 0.9 g (72%). mp 124–125°C. HRMS ($C_{17}H_{14}N_2$): 246.11459 (dev. 4.5 ppm), peaks: 231 (M-CH_3). ^1H NMR (CF_3COOD): 8.60(m, 2H), 8.55(d, 1H), 8.34(d, 1H), 7.73(t, 1H), 7.57(d, 2H), 7.42(d, 1H), 7.22(m, 3H), 2.31(s, 3H).

*2.2.4. 4-bipyridylbenzylaldehyde (**5**)*

To a solution of 0.5 M ceric ammonium nitrate in 50% aqueous acetic acid (128 ml, 64 mmol), compound **4** (2.0 g, 8 mmol) was added. The mixture was heated on a steam bath until it was pale yellow (30–60 min). The solution was cooled and then neutralized with EDTA (30 g)-ammonium hydroxide, which resulted in a yellowish suspension. If neutralized with ammonium hydroxide only, the solution was a deep red due to the coordinated complex of bipyridine and Ce(III). The suspension was extracted three times with $CHCl_3$ (50 ml), and then the combined chloroform fractions were washed with water and dried over anhydrous sodium sulfate. The yellowish chloroform solution was evaporated by rotary evaporation to obtain a sticky solid. Purification was effected on a silica gel column by flash chromatography (20 × 4.5 cm, hexane). The sample was dissolved in $CHCl_3$ and then loaded on the column. Elution was achieved with hexane–triethylamine (20 : 1), unreacted **4** was removed first followed by **5**. mp 133–134°C. HRMS ($C_{17}H_{12}N_2O$): 260.09555 (dev. 2.26 ppm), peaks: 231 (M-HCO). IR ν_{co} 1580 cm^{-1}. ^1H NMR ($CDCl_3$): 10.1(s, 1H), 8.79(dd, 1H), 8.72(d, 2H), 8.47(dt, 1H), 8.02(d, 2H), 7.93(d, 2H), 7.86(td, 1H), 7.57(dd, 1H), 7.35(dd, 1H). Each proton signal was confirmed by H–H COSY spectrum.

*2.2.5. meso-tetra-(p-(2,2′-bipyrid-4-yl)phenyl)porphyrin (**1a**)*

Anhydrous propionic acid (3 ml) was heated to 90°C in a 25 ml round bottomed flask. **5** (0.2 g, 0.77 mmol) was dissolved in the solution, and then freshly distilled pyrrole (0.05 ml, 0.77 mmol) in propionic acid (1 ml) was added. The mixture was refluxed at 130–135°C for 45 min and then cooled. The mixture was poured into a large container, water (10 ml) was added, and sufficient Na_2CO_3 was added over 1 h to bring the pH to 5 in order to deprotonate the bipyridyl groups, which precipitated the product. The resulting precipitate was collected by suction filtration, and washed with water, acetone, and hot *N*,*N*-dimethylformamide to remove a black impurity. The solid was dried at 100°C for several hours which yielded 20 mg of purple product. m.p. > 400°C. FAB/MS ($C_{84}H_{54}N_{12}$): 1231.8(100). Visible spectrum ($CHCl_3$): 422(507, 000), 518(21, 000), 554(13, 000), 592(7, 600), 650 (6, 800). ^1H NMR (CF_3COOD): 9.40(s, 4H), 9.38(2, 4H), 9.37(d, 4H), 9.10(s, 8H), 9.08(t, 4H), 9.07(d, 8H), 9.04(d, 4H), 9.01(d, 4H), 8.81(d, 8H), 8.53(t, 4H). *Anal* Calc. for $C_{84}H_{54}N_{12}\cdot H_2O$: C, 80.75; H, 4.52; N, 13.45. Found C, 80.01; H, 4.42; N, 13.66%.

The zinc substituted porphyrin (**1b**) was prepared using the literature method [12]. **1a** (0.045 g, 0.0365 mmol) was dissolved in 2 : 1 acetic acid–water (75 ml). Zinc acetate (0.168 g, 0.914 mmol) was dissolved in the same solvent (30 ml) and the two solutions were mixed and stirred in a hot water bath (45°C) for 12 h. After the reaction, the mixture was cooled to room temperature and 6 M NaOH (aq) was added until a green precipitate formed. The precipitate was collected by gravity filtration, washed with water, and dried in a vacuum oven. This yielded 0.042 g of a purple solid (89%) which has the characteristic absorption and emission spectra of a metalloporphyrin (see Table 1).

2.3. Measurements

UV–Vis spectra were recorded on a Hewlett-Packard 8451 single beam diode array spectrophotometer. Melting points (uncorrected) were obtained using an Electrothermal 9100 apparatus. NMR spectra were recorded on a GE 500 MHz spectrometer. Mass spectra at high resolution and FAB mass spectra were obtained using a Kratos Profile spectrometer. Infrared spectra were obtained as KBr disks and were recorded on a Mattson instruments Cygnus 100 FTIR. Microanalyses were done by Desert Analytics (Tucson, AZ).

Luminescence spectra were recorded using a SPEX Industries Model 111C photon counting fluorimeter equipped with a 450 W Xe arc lamp and both a cooled photomultiplier housing and a charge coupled detector. The absorbance of all solutions was less than 0.4 at the excitation wavelength.

Luminescent lifetimes of the complexes were obtained in room temperature solutions. Luminescence decays were measured by time correlated single photon counting, which system has been described elsewhere [13]. The observed decay was simulated by using convolution analysis. The observed lamp pulse is used as the excitation function and an impulse response of the proper form is assumed and fitted.

Table 1
Absorption and luminescence maxima and luminescence lifetimes of porphyrins in room temperature solutions

Compound	Solvent	Soret λ_{max} (nm)	Absorption maxima Q bands λ_{max} (nm)	Emission maxima λ_{max} (nm)	Emission lifetime[a] τ_{em} (ns)
$[H_2\mathbf{1a}]^{2+}$	2 : 1 HOAc : H_2O	448	662	711	2.4
H_2TPP	DMSO	418	514, 550, 592, 646	654, 717	12.7
1a	$CHCl_3$	422	518, 554, 592, 648	662, 726	–
1b	$CHCl_3$	428	554, 600	618, 664	–
1b	DMSO	432	562, 604	617, 664	2.0
ZnTPP	DMSO	428	560, 600	612, 663	2.5

[a]As measured by time correlated single photon counting.

The program was written in FORTRAN and run on an IBM/RS6000 system.

2.3.1. Quenching of **1a** *and* **1b** *emission by metal ions*

The glassware used in this experiment was boiled in dilute aqueous EDTA solution and rinsed well with deionized distilled water before they were dried to remove any metal ions adsorbed in the glass. Various volumes of a stock metal ion solution in DMSO were added to 1 ml of a 7.7 μM stock porphyrin solution in the same solvent, and the final volume was adjusted to 4 ml with DMSO. The solutions were mixed well before being capped and stored in the dark until emission and/or absorption spectra were taken. The integrated emission intensity was determined by taking the peak area from 575.1 to 800.1 nm.

2.3.2. Measurement of quenching rate constants

Rate constants for quenching of the porphyrin singlet were measured by picosecond kinetic spectrophotometry. Samples were excited with the doubled output of regeneratively amplified pulses from a Ti : sapphire laser (Spectra Physics Tsunami/Spitfire combination). Typical excitation pulses following doubling with BBO were between 420 and 430 nm at a frequency of 1000 Hz; pulse widths were approximately 120 fs with energies between 20 and 40 μJ. Absorbance measurements at various delays following excitation were made using continuum generated from residual 840–860 nm pulses of the regenerative amplifier. Excitation and analysis pulses were passed through a 2 mm path cell nearly colinearly and the analysis pulse was passed through a monochromator (ISA, 1/8 m) to a photodiode detector (Thor Labs). The excitation pulses were chopped such that alternate analyzing pulses included sample excitation. The photodiode output signal for each pulse was integrated using a gated integrator (SRS Model SR 250) and digitized (National Instruments AT M10 16E). Absorbance changes were then calculated from the two pulses. Typically 1000–3000 absorbance measurements were averaged at each delay and decays were collected over 200–500 delays.

3. Results and discussion

3.1. Porphyrin synthesis

The preparative method for the tetra-(bipyridylphenyl)-porphyrin (**1a**) involves only four steps and is outlined in Scheme 1. The approach involves preparation of *p*-(2,2′-bipyrid-4-yl)benzaldehyde using a modification of the Hantzsch pyridine synthesis [14] followed by reaction of the aldehyde with pyrrole by the classic Adler porphyrin synthesis [15]. Overall yields for the preparation are low, but starting materials are inexpensive and several hundred milligrams of the porphyrin could be prepared conveniently. The porphyrin is only sparingly soluble in most organic solvents, but is very soluble in mixtures of acetic acid and water, in which the protonated porphyrin, $[H_2\mathbf{1a}]^{2+}$, is the predominant chromophore in solution.

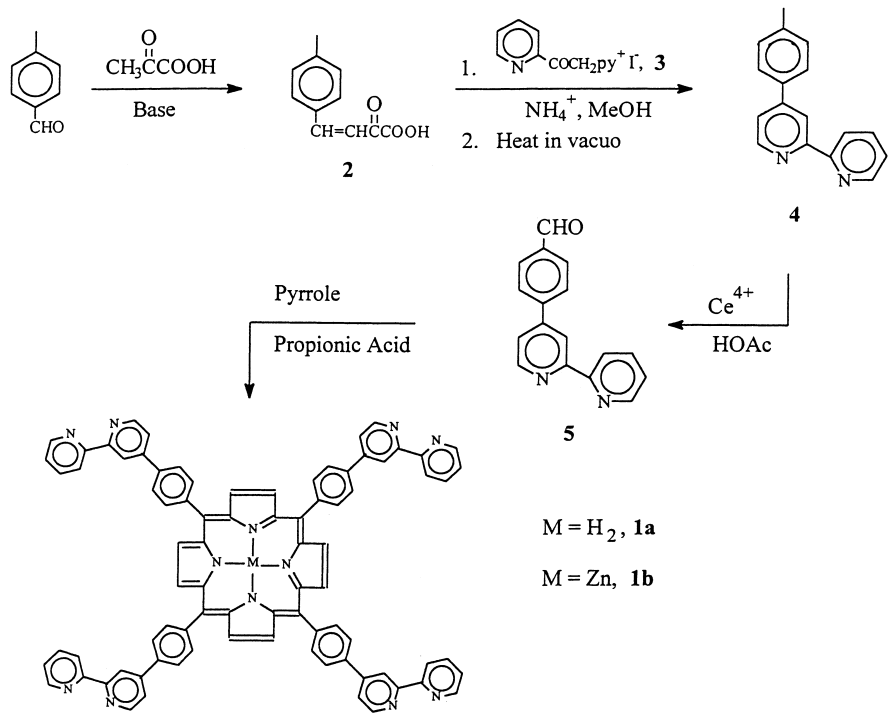

Scheme 1.

Metalation of the porphyrin with Zn(II) was performed with a large excess of $Zn(OAc)_2$ in aqueous acetic acid. The product contained the Zn(II) porphyrin (**1b**) with a mixture of metalated bipyridyl ligands. The fact that metalation of the porphyrin was complete was evidenced by the absence of free base porphyrin luminescence in emission spectra of the product (see Table 1). Quantitative analysis of the degree of Zn(II) association with **1a** was attempted using FAB mass spectrometry, but the material formed in the synthesis yields no signal from an MNBA matrix, presumably due to the formation of high molecular weight oligomers (Zn(II) linking bipyridine moieties of porphyrins). The Zn(II) porphyrin isolated is sparingly soluble in most organic solvents, but exhibits reasonable solubility in DMSO and DMSO–H_2O mixtures. As a result, quenching experiments were performed in DMSO.

3.1.1. Absorption and luminescence behavior of **1a** *and* **1b**

Table 1 lists the absorption and fluorescence maxima for the free base porphyrin, zinc porphyrin and the dication of the free base porphyrin in room temperature solutions. Data are also given for tetraphenylporphyrin and its Zn(II) complex. The Soret band exhibits a large spectral shift and the four Q bands of the free base yield only a single transition at lower energy in the doubly protonated porphyrin. Both the absorption spectra and the fluorescence spectra of **1a** and $[H_2\mathbf{1a}]^{2+}$ closely resemble the same spectra of meso-tetraphenylporphyrin, H_2TPP.

The absorption and luminescence spectra of the Zn(II) porphyrin are very similar to spectra reported for [Zn(II)TPP]. In addition, the absorption bands exhibit little solvatochromism; the spectra reported in Table 1 for DMSO and $CHCl_3$ solutions of **1b** exhibit maxima that differ by less than 10 nm for all absorption and fluorescence bands.

Fluorescence lifetimes for both **1a** in $CHCl_3$ and **1b** in DMSO are very short. Using a flashlamp based time correlated single photon counting apparatus the lifetimes are estimated to be less than 3 ns for both porphyrins. The fluorescence lifetimes of H_2TPP and ZnTPP in methylcyclohexane at room temperature are 13.6 and 2.7 ns, respectively; [16] in DMSO the lifetimes are similarly long ($H_2TPP = 12.7$ ns; $ZnTPP = 2.5$ ns). It is clear the presence of the bipyridyl substituents leads to an increase in nonradiative relaxation of the free base porphyrin. The fluorescence quantum yield of **1b** in DMSO was determined to be 0.04, twice that of ZnTPP in DMSO (0.02); since the fluorescence lifetime of **1b** is less than that of ZnTPP, the implication is that the radiative decay rate constant for **1b** is greater than ZnTPP by a factor of approximately 2.5.

3.1.2. Metal ion association with 1b and quenching of porphyrin luminescence

The relative degree of the Zn porphyrin (**1b**) luminescence quenching by several cations was examined in DMSO solutions by determining the ratio of the integrated fluorescence intensity in the absence (I_0) and presence (I) of added metal ion. The fraction of excited states quenched ($1 - I/I_0$) is given in Table 2 for solutions containing 0.1 and 1.0 mM metal ion with no added electrolyte. No luminescence quenching is observed for Na(I), Ca(II), Cr(III), Mn(II), Zn(II), Cd(II) and Pb(II), while measurable quenching (greater than 5% of total **1b** emission quenched at given concentration of added metal ion) was observed for Fe(II), Co(II), Ni(II) and Cu(II). Given the very short fluorescence lifetime of **1b**, it can readily be determined that essentially no bimolecular quenching is expected at 1 mM concentrations of added metal ions, even if the quenching rate constant is diffusion limited.[1] Thus, quenching must be the result of formation of a ground state complex between **1b** and an ion (Eq. (1)).

Table 2
Fraction of **1b** excited states quenched by various metal ions in 1 : 1 H_2O : DMSO solutions at room temperature

Metal ion	Fraction quenched 100 $(1 - I/I_0)$	
	$[M] = 10^{-4}$ M	$[M] = 10^{-3}$ M
Na(I)	0	0
Cr(III)	0	0
Mn(II)	0	0
Fe(II)	16	96
Co(II)	95	94
Ni(II)	88	88
Cu(II)	98	98
Zn(II)	0	0
Cd(II)	0	0
Hg(II)	16	13
Pb(II)	0	0

$$M^{n+} + \mathbf{1b} \xrightarrow{K_1} \{M[\mathbf{1b}]\}^{n+} \quad (1)$$

Evidence for metal ion association with the bipyridylporphyrin is also observed spectrophotometrically. Fig. 2 shows absorption changes in the Soret band of **1b** (420 nm) in the presence of varying concentrations of Cu(II) and Zn(II). The absorptivity of the Soret band decreases and the full width at half maximum increases upon addition of M(II). For Cu(II) the FWHM of the absorption band increases from 12 to 20 nm upon addition of 13 μM Cu(II) to a 10^{-7} M solution of **1b**, while smaller changes are observed upon addition of Zn(II). The porphyrin Q bands at 560 and 605 nm are unaffected by the addition of ions to the solution. The spectrophotometric changes were not investigated in detail, but the observed change may be due to lowering of the symmetry of the porphyrin, giving rise to a set of Soret bands of nearly equal energy for **1b** bound to one, two, three and four M(II) ions.

The absence of quenching for Na^+ and Zn^{2+} is not surprising since these ions are not easily oxidized or reduced, the solvated ions have no low energy excited states

[1] Assuming Stern–Volmer quenching kinetics with a value for k_{diff} of 10^{10} M^{-1} s^{-1} and a singlet lifetime of 2.5 ns.

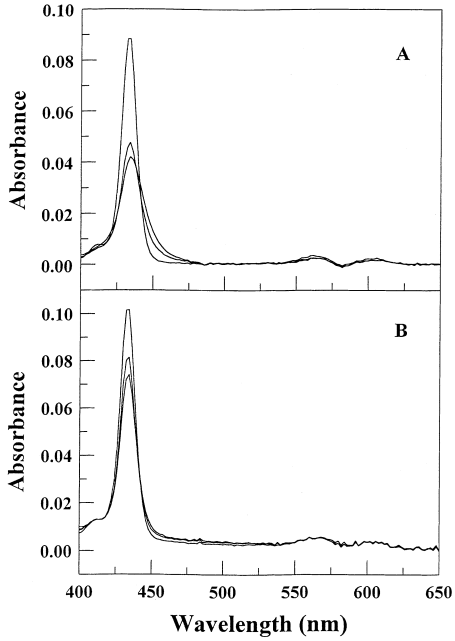

Fig. 2. Spectrophotometric changes observed upon addition of (A) Cu(II) at concentrations of 0, 4.4 and 13 μM and (B) Zn(II) at concentrations of 0, 0.25 and 0.63 mM to solutions of **1b** in DMSO.

and their spin orbit coupling constants are small enough that they should not significantly affect the rate constant for intersystem crossing from the singlet excited state of **1b**.

In contrast, both Cr(III) and Mn(II) have ligand field excited states that are lower in energy than the porphyrin excited singlet (approximately 2.0 eV for **1b**) and energy transfer quenching is possible. $[Cr(III)(OH_2)_6]^{3+}$ has a ^4T excited state that is approximately 2.0 eV above the ground state and a ^2E state that is at approximately 1.8 eV [17]. The ligand field state energies of Cr(III) coordinated to the bipyridyl of **1b**, of course, will differ in energy; it is known that the energy of the ^4T state of $[Cr(bpy)_3]^{3+}$ is approximately 2.6 eV [18] and the doublet states (^2E and ^2T) are 1.7 eV above the ground state [19]. Since the ground state of Cr(III) is a quartet, energy transfer is spin allowed only for transfer from the singlet excited state of the porphyrin to the quartet excited; however, this energy transfer process is likely to be energetically unfavorable.

With Mn(II), the ground state of aqueous and DMSO solutions is a sextet [17]. All low energy electronic transitions are spin forbidden and energy transfer from the porphyrin singlet to Mn(II) is also forbidden. Since only very strong field ligands such as CN^- yield spin paired Mn(II) complexes, it is likely that Mn(II) coordinated to the bipyridyl moiety of **1b** will also have a sextet ground state and thus have spin forbidden energy transfer.

Photoinduced electron transfer reactions involving the excited singlet of **1b** and Cr(III) may also be possible. The thermodynamic potential for reduction of Cr(III) in aqueous solutions is −0.75 V versus SCE and that of $[Cr(III)(bpy)_3]^{3+}$ is −0.25 V [20,21]. The potential for oxidation of the excited state **1b** can be approximated from the excited state energy and potential for one electron oxidation. Because of the limited solubility of **1b** reliable one electron redox potentials were not accessible and the literature value for the ZnTPP(+)/ZnTPP(0) potential was used to estimate the excited state potential [22]. Using the measured excited state energy of **1b** and the literature redox value, the potential for the reduction of the cation to yield the excited state is approximately −1.2 V versus SCE:

$$[\mathbf{1b}]^+ + e^- \rightarrow [\mathbf{1b}]^* \qquad E(+/^*)_{\mathbf{1b}} \sim -1.2\,\text{V versus SCE}$$

From the potentials, it is clear that photoreduction of Cr(III) is thermodynamically favorable regardless of the coordination environment of the Cr(III). Possible explanations for the absence of observable quenching for Cr(III) are (a) a low formation constant for Cr(III) association with the bipyridyl porphyrin or (b) electron transfer kinetics which are slow on the time scale of the fluorescence decay. Using available formation constants for complexation of 2,2′-bipyridine by various divalent and trivalent metal ions as a guide [21], it is expected that, at Cr(III) concentrations of 1 mM and **1b** concentrations of 10 μM, greater than 90% of the **1b** in solution should have coordinated at least one Cr(III) ion. Thus, the most likely reason that electron transfer quenching by Cr(III) is not observed is that the rate constant for the intramolecular reduction is much slower than the relaxation of the singlet state of the porphyrin. Among the other non-quenching or weakly quenching ions, Hg(II), Cd(II) and Pb(II) have formal reduction potentials that are accessible, but these are all two electron potentials. Since the quenching must occur via an intramolecular reaction, the appropriate potentials needed to determine the free energy for photoreduction of the metal ions are for reduction of $[(bpy)M(n^+)(OH_2)_4]^{n+}$ or related complexes, which are not available.

The excited state of the porphyrin may also act as a one electron oxidant. For complex **1b** the potential for reduction of the singlet state is:

$$[\mathbf{1b}]^* + e^- \rightarrow [\mathbf{1b}]^- \qquad E(*/-) \sim 0.7\,\text{V versus SCE}$$

In principle, the excited porphyrin could serve as an oxidant for Mn(II), Fe(II), Co(II) and Pb(II). The potential for one electron oxidation of $[Mn(II)(OH_2)_6]^{2+}$ is very negative and the one electron oxidation of Pb(II) must be at potentials more positive than the potential for the two electron process. The $[Fe(III/II)(OH_2)_6]$ potential is 0.53 V versus SCE while the $[Fe(III/II)(bpy)_3]$ potential is 0.87 V [20]. The implication is that photooxidation of Fe(II) bound to **1b** to yield an $[(S)_4Fe(II)(bpy)]^{2+}$ coordination environment should be favorable. For Co(II) the data are clear since the $[Co(III/II)(OH_2)_4(bpy)]$ potential is has been measured to be 0.60 V versus SCE; [23] photooxidation of coordinated Co(II) by excited **1b** is slightly exergonic.

From the above discussion it is clear that the ions observed to quench the emission of **1b** can do so by a variety of mechanisms. It is also of value to examine the

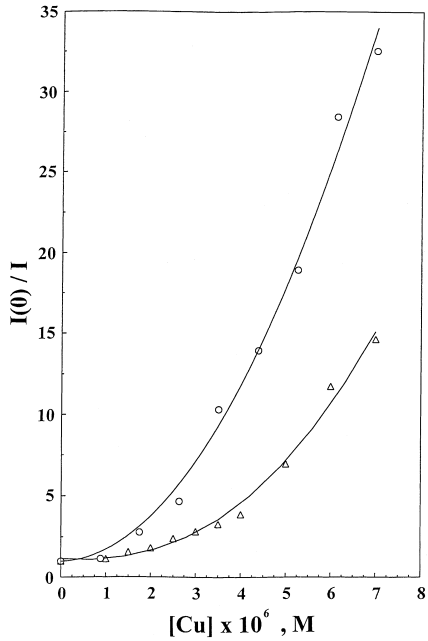

Fig. 3. Quenching of **1b** luminescence by Cu(II) in DMSO at room temperature at **1b** concentrations of 2×10^{-7} (▽) and 2×10^{-6} M (○). Solid line represents a fit to data obtained at 2×10^{-7} M **1b** where the [Cu(II)] is in large excess.

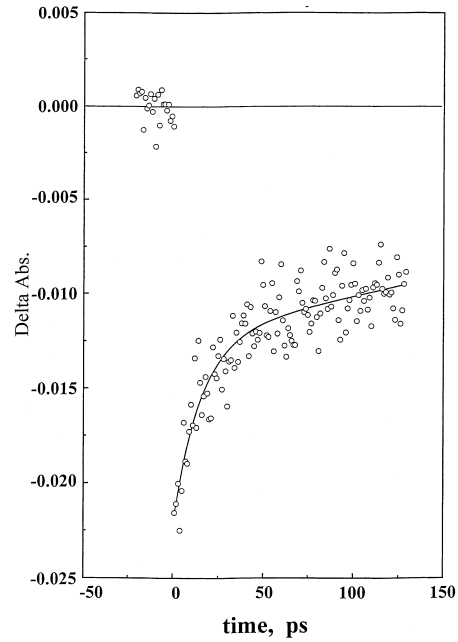

Fig. 4. Transient absorbance at 490 nm following excitation with a ca. 150 fs pulse centered at 430 nm.

association equilibria and quenching processes observed for Cu(II), Co(II) and Ni(II) in more detail. Analysis of static quenching data provide information on association equilibrium constants (Eq. (1)). In addition, picosecond time resolved transient absorption experiments provide a measure of the rate constant of the intramolecular quenching processes.

3.1.3. Quenching of **1b** *with Cu(II)*

Fig. 3 shows the Stern–Volmer Quenching ratio, $I(0)/I$, for quenching of **1b** by Cu(II) in DMSO solution at two concentrations of **1b**. An excitation wavelength of 560 nm was used for all static quenching experiments to avoid complications due to changes in porphyrin absorbance upon metal ion association. Since quenching is observed at micromolar concentrations of Cu(II) and the degree of quenching depends on the *porphyrin* concentration, it is clear that quenching is exclusively due to ground state complex formation between **1b** and Cu(II). For Cu(II), complex formation is essentially complete within 30 s of mixing with **1b**. Examination of the luminescence decay of **1b** in solutions containing varying concentrations of Cu(II) reveals that the lifetime measured by time correlated single photon counting (limited to lifetimes greater than approximately 2 ns) is invariant, as expected for a quenching process involving ground state complex formation leading to a non-emissive complex.

Picosecond time resolved absorbance measurements indicate the decay of the porphyrin singlet excited state becomes double exponential in solutions containing Cu(II). Fig. 4 shows a decay obtained following excitation at 430 nm (into the Soret band of the porphyrin). The rapid decay of the porphyrin singlet absorption at 470 nm ($\tau \approx 20$ ps) is only observed in the presence of Cu(II) and is representative of the quenching process. Given the 2.0 ns lifetime of **1b** in the absence of Cu(II), the decay rate in the presence of Cu(II) indicates that the Cu(II) **1b** complex has an emission quantum yield approximately 1% that of the uncomplexed porphyrin. The rate constant for the quenching process can be approximated as the difference between the decay rate constant of the uncomplexed porphyrin, **1b** ($1/\tau_0$), and the mono-Cu(II) complex ($1/\tau_M$, Eq. (2)). The quenching rate constant obtained in this way is 5×10^{10} s^{-1}.

$$k_q = \frac{1}{\tau_\mu} - \frac{1}{\tau_0} \tag{2}$$

From these results, it appears that a simple equilibrium expression like Eq. (1) could be used to explain the luminescence quenching behavior. For cases where the concentration of Cu(II) is much larger than that of **1b** and it is assumed that the {Cu(II)**1b**} complex is non-emissive, the Stern–Volmer quenching ratio $I(0)/I$ is linearly related to the total Cu(II) concentration.[2] Fig. 3 shows that this is clearly not the case. To fit the data in cases where there is a large excess of Cu(II) it is necessary to include the

[2]The linear relationship results from a simple equilibrium analysis of ion association for the case where the Cu(II) concentration is much larger than the luminescent porphyrin concentration. In this case the fraction of Cu(II)**1b** in solution is linearly related to the total Cu(II) concentration. Since the Cu(II)**1b** complex is assumed to be nonemissive, the ratio $I(0)/I$ equals $[\mathbf{1b}]T/[\mathbf{1b}]_{eq}$.

equilibrium for formation of a bis-copper complex, $\{Cu_2[\mathbf{1b}]\}^{4+}$ (Eq. (3)).

$$\{Cu[\mathbf{1b}]\}^{2+} + Cu(II) \overset{K_2}{\rightarrow} \{Cu_2[\mathbf{1b}]\}^{4+} \quad (3)$$

By including the additional equilibrium and accounting for the 1% relative luminescence from the mono-copper complex $\{Cu[\mathbf{1b}]\}^{2+}$, the Stern–Volmer quenching ratio is given by Eq. (4). The α terms represent the fractions of **1b** and Cu**1b** in solution at equilibrium and D is the emission yield of Cu**1b** relative to **1b** (ϕ_M/ϕ_0). Parameters obtained using Eq. (4) to fit the data shown in Fig. 3 are $5.6 \times 10^4\ M^{-1}$ for K_1 and $1.2 \times 10^7\ M^{-1}$ for K_2.

$$\frac{I(0)}{I} = (\alpha_{\mathbf{1b}} + D\alpha_{\{Cu\mathbf{1b}\}})^{-1} \quad (4)$$

where

$$\alpha_{\mathbf{1b}} = [1 + K_1[Cu(II)] + K_1K_2[Cu(II)]^2]^{-1}$$
$$\text{and } \alpha_{\{Cu\mathbf{1}b\}} = K_1\alpha_{\mathbf{1b}}[Cu(II)]$$

The values obtained for K_1 and K_2 have large margins of error (>100%), but the results clearly indicate that (a) a single binding equilibrium is not adequate to fit the data (predicts a linear equation) and (b) the inclusion of a second association does serve to explain the upward curvature in the Stern–Volmer quenching plots. These results also provide a quantitative illustration of how the presence of multiple substrate binding sites on the chromophore-receptor system serves to lower the detection limit of the system (increase the sensitivity).

The mechanism of quenching of **1b** by Cu(II) could be by either energy or electron transfer. Solutions of Cu(II) in DMSO containing 2,2′-bipyridine in 1 : 1 stoichiometry have absorption transitions in the visible which overlap the fluorescence of **1b**, suggesting the possibility of Förster energy transfer. Estimates of the Förster transfer rate constant were obtained using the quantum yield and radiative decay rate constant of **1b**, the solvent refractive index, an approximate separation distance of the porphyrin and Cu(II) complex chromophores and the overlap of the **1b** fluorescence and the Cu(II) complex absorption [24]. The estimated rate constant of $8 \times 10^8\ s^{-1}$ is much lower than the experimental rate constant for the quenching process. This result suggests that the quenching is by either exchange energy transfer or electron transfer. Fig. 4 shows that the quenching process leads to a transient having a lifetime of several ns; Zn(II) porphyrin cation radicals are known to absorb at the wavelength used in this experiment [25]. If quenching had resulted in the formation of a low energy ligand field state on the coordinated Cu(II) bipyridyl complex, it is unlikely a transient having high molar absorptivity at 490 nm would be formed. Thus, while the present data are not definitive, the most likely quenching process is electron transfer from the excited singlet of **1b** to Cu(II). We are currently investigating this in greater detail.

3.1.4. Quenching with Co(II) and Ni(II) in DMSO

Figs. 5 and 6 show Stern–Volmer curves for quenching of **1b** luminescence with Ni(II) and Co(II), respectively. For the case in which the concentration of metal ion is in large excess ($[\mathbf{1b}] = 10^{-7}$ M), the data were fit using the same ground state equilibrium approximation as that shown above for Cu(II) quenching (Eq. (4)). Table 3 lists equilibrium constants obtained from fits to Eq. (4) using fixed values for relative quenching of the mono-metalated complex (D in

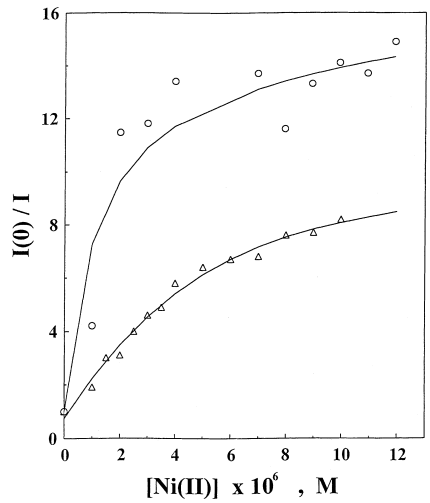

Fig. 5. Quenching of **1b** luminescence by Ni(II) in DMSO at room temperature at **1b** concentration of 2×10^{-7} M (▽) and 2×10^{-6} M (○). Solid line represents a fit to data obtained at 2×10^{-7}.

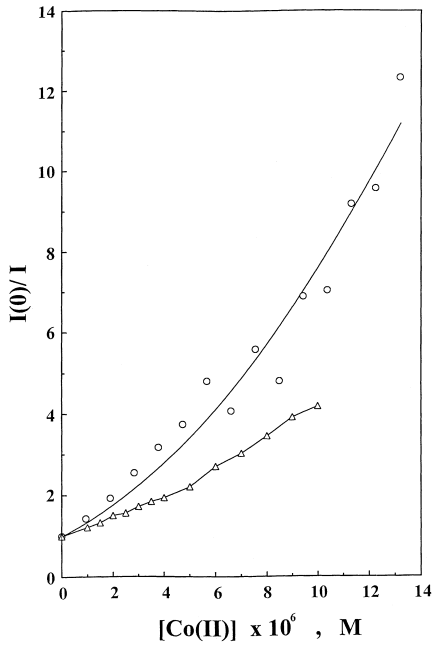

Fig. 6. Quenching of **1b** luminescence by Co(II) in DMSO at room temperature at **1b** concentration of 2×10^{-7} M (▽) and 2×10^{-6} M (○). Solid line represents a fit to data obtained at 2×10^{-7}.

Table 3
Equilibrium constants for association of one and two M(II) ions with bipyridyl moieties of **1b** obtained from fits of luminescence quenching data in DMSO solution at room temperature

Metal ion	K_1 (M^{-1})	K_2 (M^{-1})	$k_q \times 10^{-9}$ (s^{-1})
Cu(II)	6×10^4	1×10^7	50
Co(II)	3×10^5	1×10^5	50[a]
Ni(II)	3×10^4	3×10^8	7

[a]Estimated from the fits of static quenching data.
The rate constant for intramolecular quenching obtained from picosecond transient absorbance measurements is also given.

Eq. (4)). The value of the quenching rate constant is calculated from the fractional emission yield of the mono-metalated complex used to fit the luminescence quenching data and the excited state decay rate constant of **1b** ($1/\tau_0$, Eq. (2)) and is also included in the table. Fits of the Ni(II) quenching data are optimized when K_2 is greater than K_1, a non-intuitive result, while the parameters obtained for Co(II) quenching yield binding constants which differ by only a factor of 3. We are presently investigating ion binding for luminescent chromophore-receptor systems having one and two bipyridyl receptor groups per chromophore.

The quenching curves for Ni(II) and Co(II) illustrate additional modes of quenching behavior which can be observed in systems of this type. While Ni(II) has a large equilibrium constant for association, the quenching rate constant is small enough that significant porphyrin emission is observed even when fully complexed to Ni(II) (Fig. 5). In contrast, the Co(II) complex has a much larger quenching rate constant (no plateau is observed in the quenching data, Fig. 6) but the lower equilibrium constant for association is observed by the fact that higher concentrations of Co(II) are required to achieve the same degree of quenching as the Cu(II) complex. Thus, some degree of selectivity is obtained through the combination of quenching rate constants and association equilibrium constants.

The mechanism of quenching for Co(II) very likely involves reduction of the excited porphyrin as discussed above, although exchange energy transfer cannot be ruled out since the most likely quenching chromophore, Co(II)-(bpy)$(DMSO)_4$, should have ligand field states lower in energy than the porphyrin singlet state. In the case of Ni(II), one electron transfer either to Ni(III) or to Ni(I) is likely to be thermodynamically unfavorable for the Ni(II)(bpy)$(DMSO)_4$ quenching complex. This complex also should have ligand field excited states lower in energy than the singlet state of **1b**. We are presently investigating the mechanism of the quenching process using picosecond time resolved absorption spectrophotometry.

4. Summary

This work presents the photophysical characterization of the Zn(II) porphyrin **1b** in DMSO solutions at room temperature. The porphyrin has four bipyridyl substituents capable of binding metal ions and the porphyrin luminescence is readily quenched by low concentrations of Cu(II), Ni(II) and Co(II) in solution via formation of a ground state complex which will undergo energy or electron transfer upon excitation. Analysis of luminescence quenching of **1b** by Cu(II) served to illustrate that the presence of multiple metal ion binding sites on luminescent sensor chromophores can have a large impact on the concentration dependence of the degree of quenching.

The key factors determining whether luminescence quenching is observed are the equilibrium constant for metal ion binding and the relative rate constant for quenching by the metal ion bound to the porphyrin. Since rate constants for intramolecular energy and electron transfer reactions depend intimately on the magnitude of electronic coupling through the covalent bridge linking the chromophore to the quenching moiety, it should be possible to achieve some degree of selectivity in sensing particular metal ions by tuning the electronic coupling via synthetic design.

Acknowledgements

The authors would like to acknowledge the Department of Energy, Office of Basic Energy Sciences (Grant DE-FG-02-96ER14617) and the Tulane Center for Photoinduced Processes, funded by the National Science Foundation and the Louisiana Board of Regents for support of this work. RAK wishes to thank the Louisiana Board of Regents for Graduate Fellowship support.

References

[1] M.J.P. Leiner, Anal. Chim. Acta 255 (1991) 209.
[2] L. Fabbrizzi, A. Poggi, Chem. Soc. Rev. 24 (1995) 197.
[3] R.A. Bissell, A.P. de Silva, G.H.Q. Nimal, Chem. Soc. Rev. 21 (1992) 187.
[4] M.A. Mortellaro, D.G. Nocera, Chemtech 2 (1996) 17.
[5] R.A. Bissell, A.P. deSilva, H.Q.N. Gunaratne, P.L.M. Lynch, G.E.M. Maguire, C.P. McCoy, K.R.A. Sandanayake, Top. Curr. Chem. 168 (1993) 223.
[6] V. Ramamurthy, D.F. Eaton, J.V. Caspar, Acc. Chem. Res. 25 (1992) 299.
[7] C.L. Exstrom, J.R. Sowa, C.A. Daws, D. Janzen, K.R. Mann, Chem. Mater. 7 (1995) 15.
[8] C.A. Daws, J.C. Vickery, M.M. Olmstead, E.Y. Fung, A.L. Balch, Angew. Chem., Int. Ed. Engl. 36 (1997) 1179.
[9] M.A. Mansour, W.B. Connick, R.J. Lachicotte, H.J. Gysling, R. Eisenberg, J. Am. Chem. Soc. 120 (1998) 1329.
[10] K.B. Wiberg, Oxidation in Organic Chemistry, Part A, Academic Press, New York, 1965, p. 271.
[11] F. Krohnke, U.F.K. Gross, Chem. Ber. 92 (1959) 22.
[12] A.D. Adler, F.R. Longo, W. Shergalis, J. Am. Chem. Soc. 86 (1964) 3145.
[13] E. Taffarel, S. Chirayil, W.Y. Kim, R.P. Thummel, R.H. Schmehl, Inorg. Chem. 35 (1996) 2127.
[14] F. Krohnke, Synthesis 1 (1976) 1.

[15] A.D. Adler, F. Longo, J. Finarelli, J. Assour, L. Korsakoff, J. Org. Chem. 32 (1967) 476.
[16] A. Harriman, J.C.S. Faraday I 76 (1980) 1978.
[17] B. Figgis, Introduction to Ligand Fields, Wiley-Interscience, New York, Chap. 9, 1966.
[18] M. Maestri, F. Bolletta, L. Moggi, V. Balzani, M.S. Henry, M.Z. Hoffman, J. Am. Chem. Soc. 100 (1978) 2694.
[19] N. Serpone, M.Z. Hoffman, J.Chem. Educ. 60 (1983) 853.
[20] K. Niki, in: A.J. Bard, R. Parsons, J. Jordan (Eds.), Standard Potentials in Aqueous Solution, Dekker, New York, 1985, pp. 453–461.
[21] W.R. McWhinnie, J.D. Miller, Adv. Inorg. Chem. Radiochem. 12 (1969) 135.
[22] K.M. Smith, Porphyrins and Metalloporphyrins, Elsevier, New York, 1975, pp. 601–602.
[23] F. Farina, R.G. Wilkins, Inorg. Chem. 7 (1968) 514.
[24] J.A. Barltrop, J.D. Coyle, Principles of Photochemistry, Wiley, New York, 1978.
[25] H. Imahori, K. Hagiwara, M. Aoki, T. Akiyama, S. Taniguchi, T. Okada, M. Shirakawa, Y. Sakata, J. Am. Chem. Soc. 118 (1996) 11771.